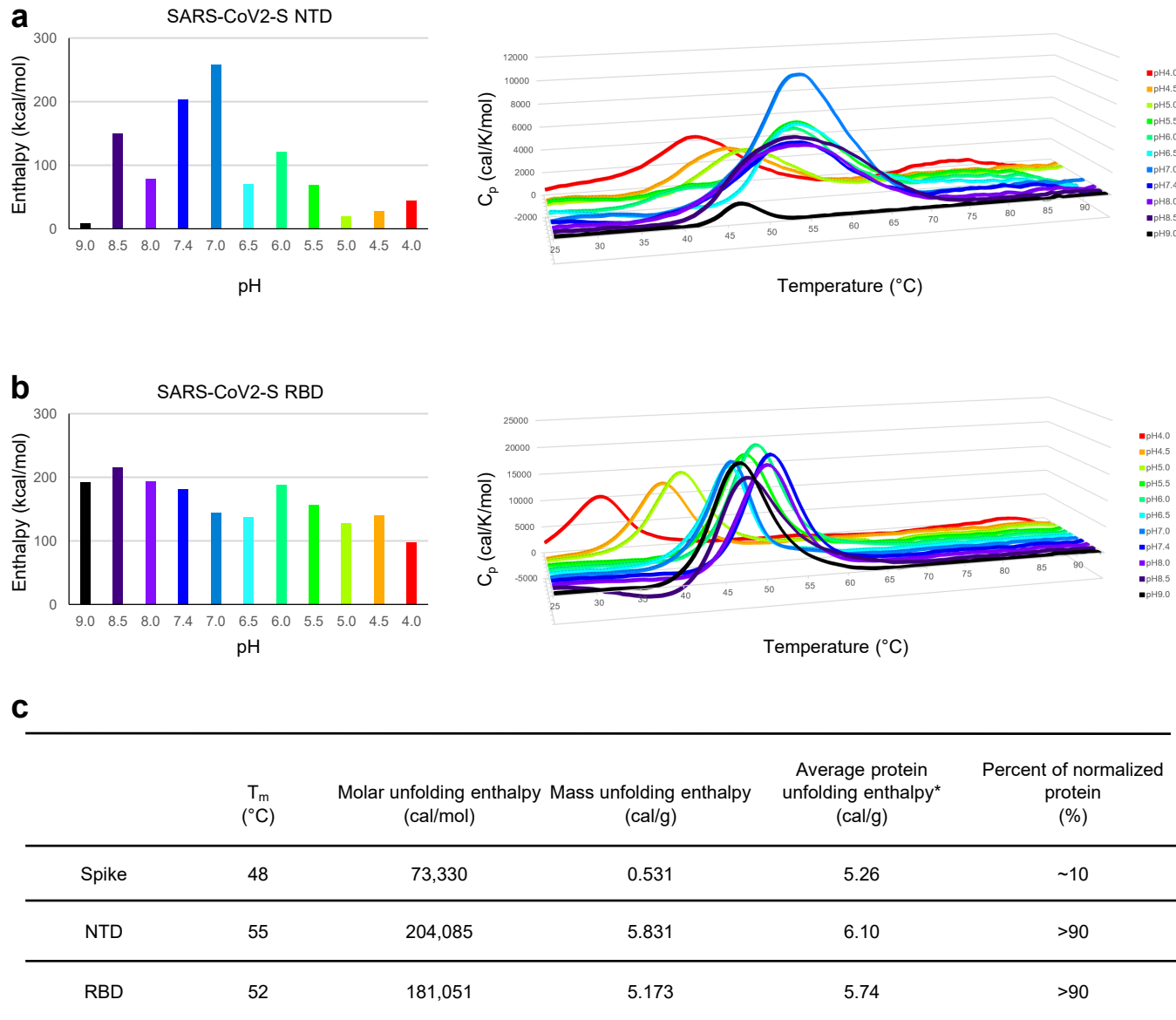


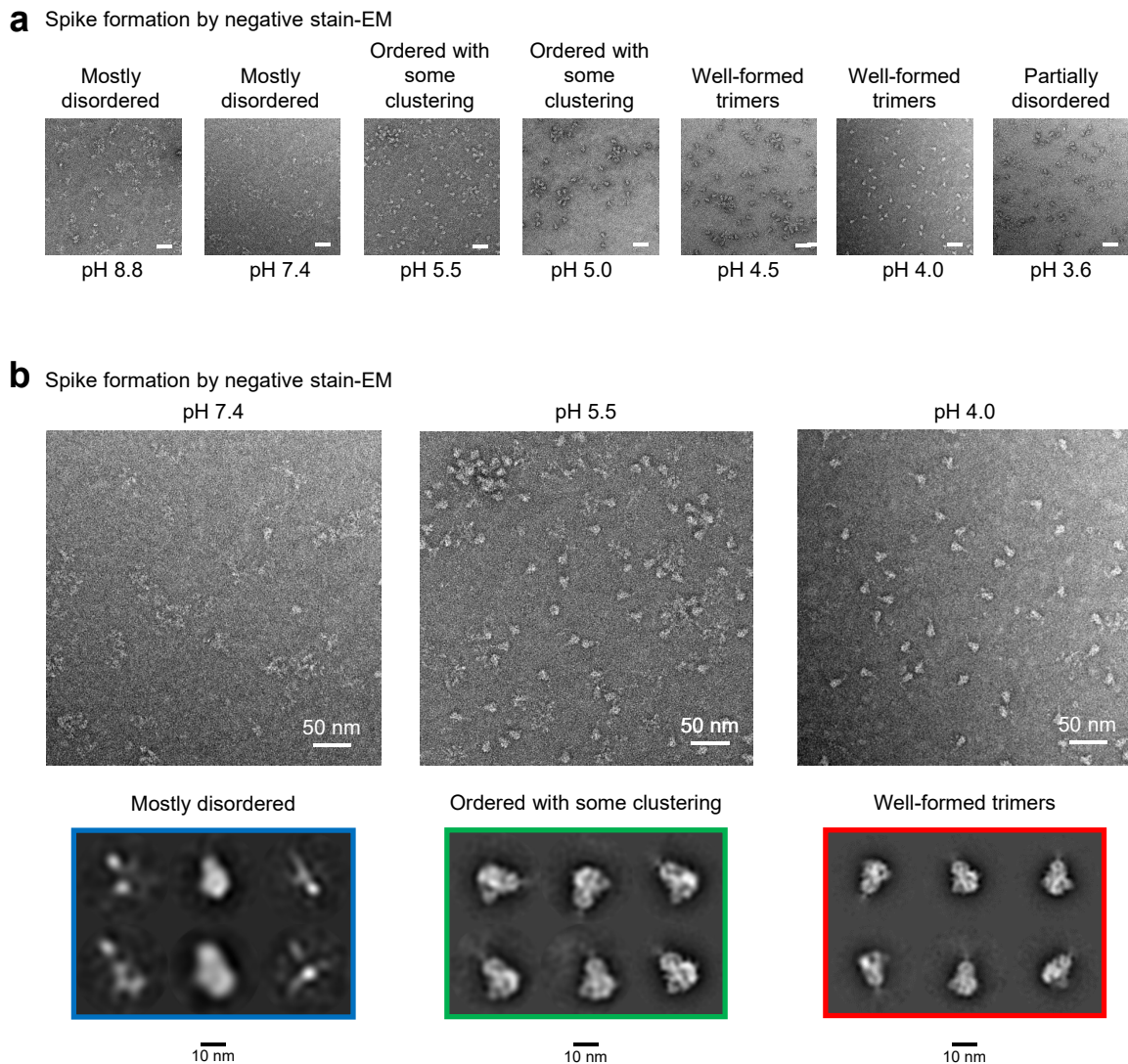
Extended Data Figure 1



* Calculated by $\Delta H = \Delta H_{ref} + \Delta C_p(T-T_{ref})$ where $T_{ref}=60^\circ\text{C}$, $\Delta H_{ref}=6.7\text{ cal/g}$, and $\Delta C_p=0.12\text{ cal/K/g}$

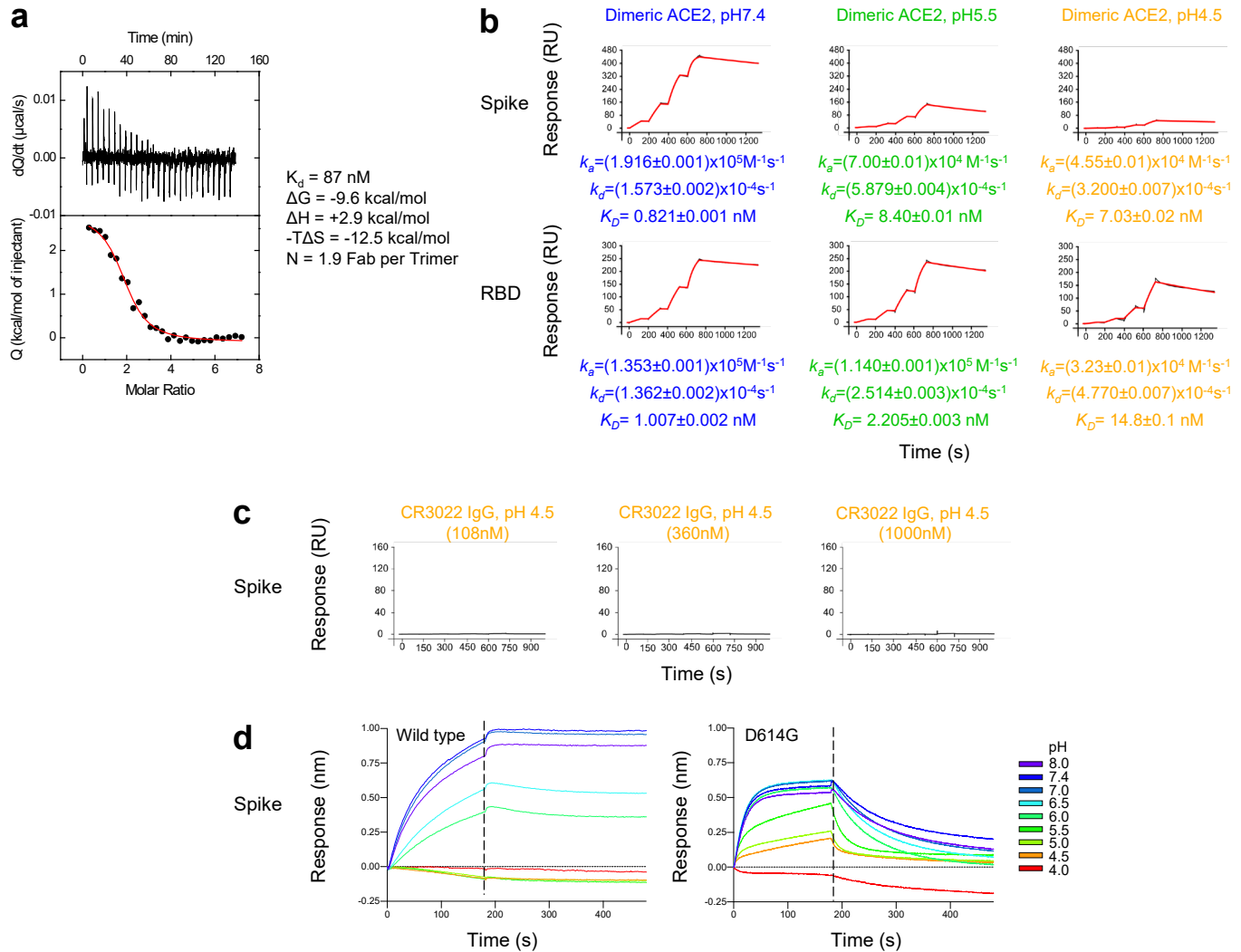
Extended Data Figure 1 | Unfolding enthalpy of SARS-CoV-2 NTD and RBD as a function of pH. **a**, DSC denaturation curves for SARS-CoV-2 NTD. **b**, DSC denaturation curves for SARS-CoV-2 RBD. **c**, Calculations of normalized unfolding enthalpy relative to that of an average globular protein. The enthalpy of unfolding of the spike protein is considerably smaller than expected at pH 7.4 and above. The thermal unfolding of the spike at pH 7.4 has its main transition centered at 48 °C with an overall enthalpy of unfolding of 73.3 kcal/mol or 0.531 cal/g, which is about an order of magnitude smaller than expected for a protein of this size. In comparison, the expected unfolding enthalpy for the average globular protein is about 5.3 cal/g at this temperature (obtained after extrapolation from 60 °C, where the enthalpy and heat capacity changes for the unfolding of the average globular protein are 6.7 cal/g and 0.12 cal/(K × g), respectively [see Methods and Robertson, A. D., and Murphy, K. P. (1997) Chem. Rev., 97, 1251-1267]).

Extended Data Figure 2



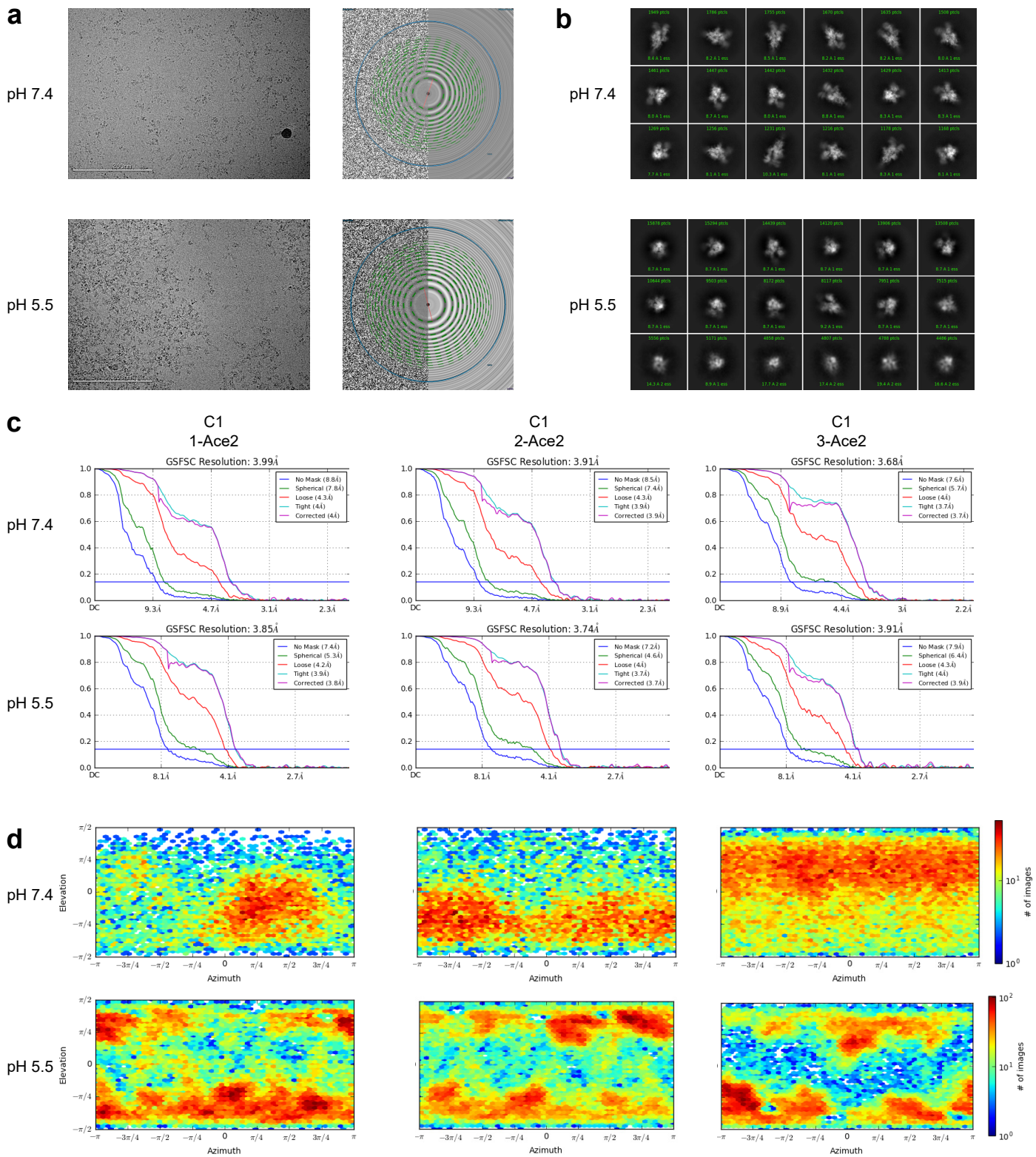
Extended Data Figure 2 | Negative stain EM indicates SARS-CoV-2 to be partially folded at physiological pH and to assemble into highly ordered trimers at endosomal pH. Negative stain-EM assessment of spike folding versus pH. **a**, Typical micrographs in the 3.6–8.8 pH range. Scale bars are 50 nm long. **b**, Close-up views and 2D-class averages for pH 7.4, 5.5, and 4.0.

Extended Data Figure 3



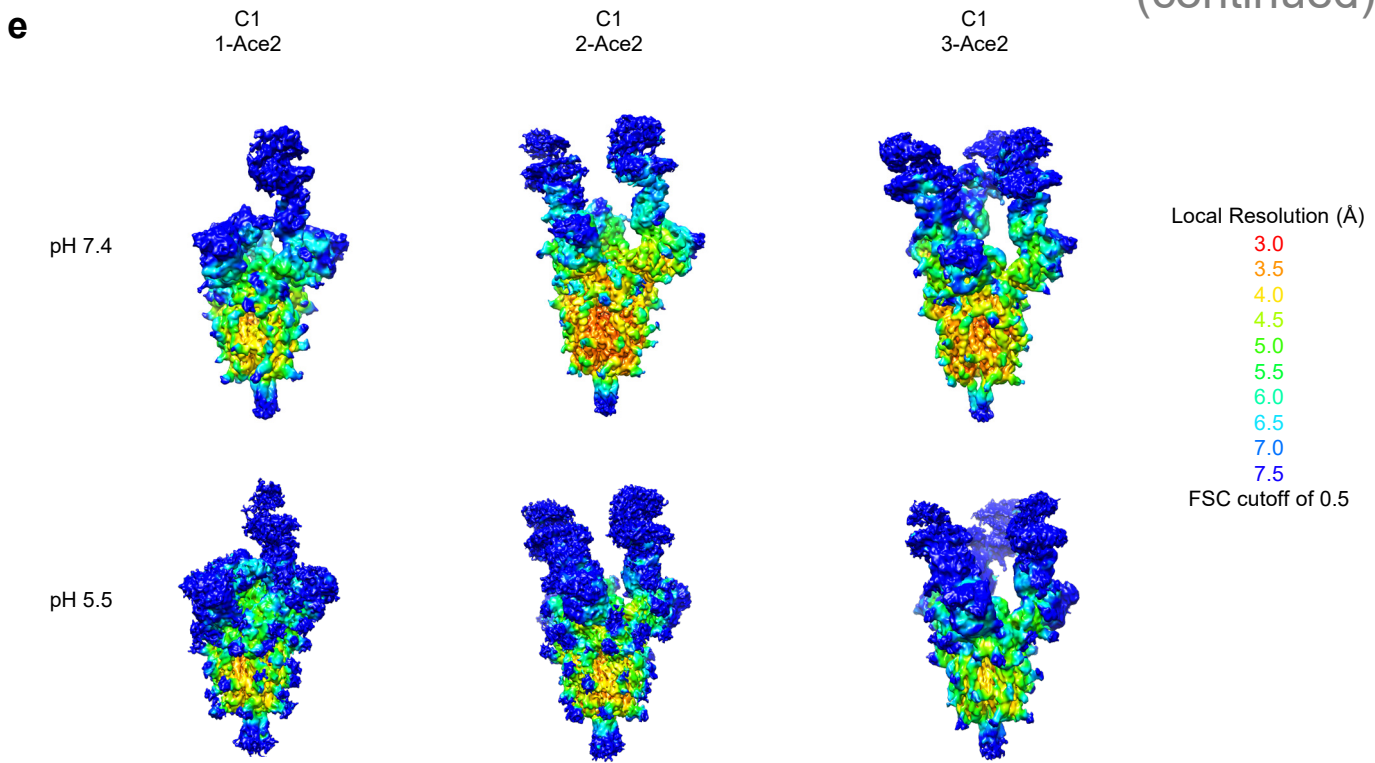
Extended Data Figure 3 | Isothermal titration calorimetry, surface plasmon resonance, and bio-layer interferometry of SARS-CoV-2 spike binding to antibody CR3022 and ACE2 receptor. **a**, Isothermal titration calorimetry of SARS-CoV-2 spike with Fab CR3022 at pH 7.4 and 25 °C. The thermodynamic binding parameters together with the stoichiometry are shown to the right. **b**, SPR single-cycle kinetics for dimeric ACE2 binding over biotinylated spike (top) and biotinylated-RBD (middle) each tethered to a chip surface. Black traces represent the experimental data and red traces represent the fit to a 1:1 interaction model. The error in each measurement represents the error of the fit. **c**, SPR single cycle kinetics for CR3022 IgG binding to the spike at pH 4.5 performed at higher concentration series, 4 to 108 nM (left), 13.33 to 360 nM (middle) and 37.04 to 1000 nM (right). **d**, Bio-Layer Interferometry assay of CR3022 IgG binding to SARS-CoV-2 spike and its D614G mutant. Antibody was loaded onto anti-human-Fc sensors and then dipped into spike protein solutions at different pH.

Extended Data Figure 4



Extended Data Figure 4 | CryoEM with ACE2 at pH 7.4 and 5.5. **a**, Representative micrographs at pH 7.4 (top) and 5.5 (bottom) are shown along with corresponding CTF. **b**, Representative 2D-class averages are shown for each pH. **c**, The gold-standard Fourier shell correlation is shown for each complex at both pH 7.4 and 5.5 using non-uniform refinement. **d**, The orientations of all particles used in the final refinement are shown as a heatmap. *(continued on next page)*

Extended Data Figure 4 (continued)

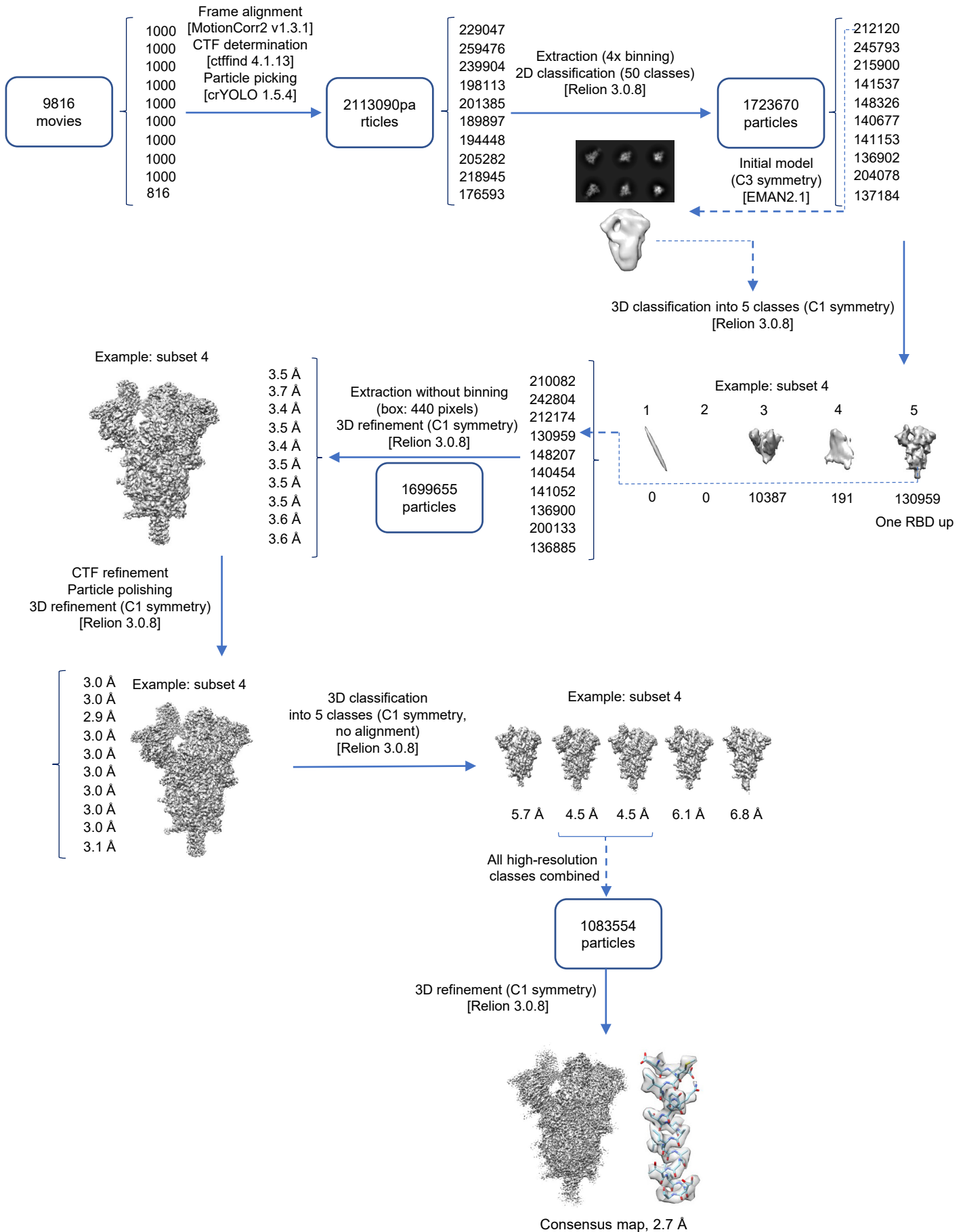


f **Cryo-EM data collection, refinement and validation statistics**

	SARS-CoV-2 spike with single ACE2 at pH 7.4	SARS-CoV-2 spike with double ACE2 at pH 7.4	SARS-CoV-2 spike with triple ACE2 at pH 7.4	SARS-CoV-2 spike with single ACE2 at pH 5.5	SARS-CoV-2 spike with double ACE2 at pH 5.5	SARS-CoV-2 spike with triple ACE2 at pH 5.5
Data collection and processing						
Magnification	81,000	81,000	81,000	81,000	81,000	81,000
Voltage (kV)	300	300	300	300	300	300
Electron exposure (e-/Å ²)	53.49	53.49	53.49	51.3	51.30	51.3
Defocus range (μm)	-0.4 to -3.6	-0.4 to -3.6	-0.4 to -3.6	-0.2 to -3.7	-0.2 to -3.7	-0.2 to -3.7
Pixel size (Å)	1.058	1.058	1.058	1.058	1.058	1.058
Symmetry imposed	C1	C1	C1	C1	C1	C1
Initial particle images (no.)	541,541	541,541	541,541	571,986	571,986	571,986
Final particle images (no.)	16,997	48,008	42,947	46,714	55,297	47,386
Map resolution (Å)	3.99	3.91	3.68	3.85	3.74	3.91
FSC threshold	0.143	0.143	0.143	0.143	0.143	0.143
Map resolution range (Å)	444.4-3.99	444.4-3.91	444.4-3.68	406.3-3.85	406.3-3.74	406.3-3.91
Refinement						
Initial model used (PDB code)	6VXX, 6M0J					
Model resolution (Å)	3.9	3.7	3.7	4.1	4	4.1
FSC threshold	0.143	0.143	0.143	0.143	0.143	0.143
Map sharpening <i>B</i> factor (Å ²)	-111.6	-94.2	-72.2	-60.3	-55.4	-51.3
Model composition						
Non-hydrogen atoms	28110	32784	39741	27320	31342	39069
Protein residues	3589	4165	4887	3512	4123	4887
Ligands	12	52	78	12	42	64
<i>B</i> factors (Å ²)(mean)						
Protein	96.3	104.25	144.2	140.5	143.7	180.1
Ligand	182.7	113.6	155.9	193.2	168.2	218.9
R.m.s. deviations						
Bond lengths (Å)	0.007	0.003	0.004	0.008	0.009	0.004
Bond angles (°)	0.843	0.697	0.0795	1.128	1.076	0.877
Validation						
MolProbity score	1.46	1.43	1.58	2.71	2.1	1.6
Clash score	4.44	4.3	4.63	6.42	5.42	4.93
Poor rotamers (%)	0.14	0	0.07	0.12	0.98	0.02
Ramachandran plot						
Favored (%)	94.4	96.57	94.7	92.9	94.5	95.09
Allowed (%)	5.4	3.43	5.28	7.1	5.5	4.85
Disallowed (%)	0.1	0	0.02	0	0	0.06

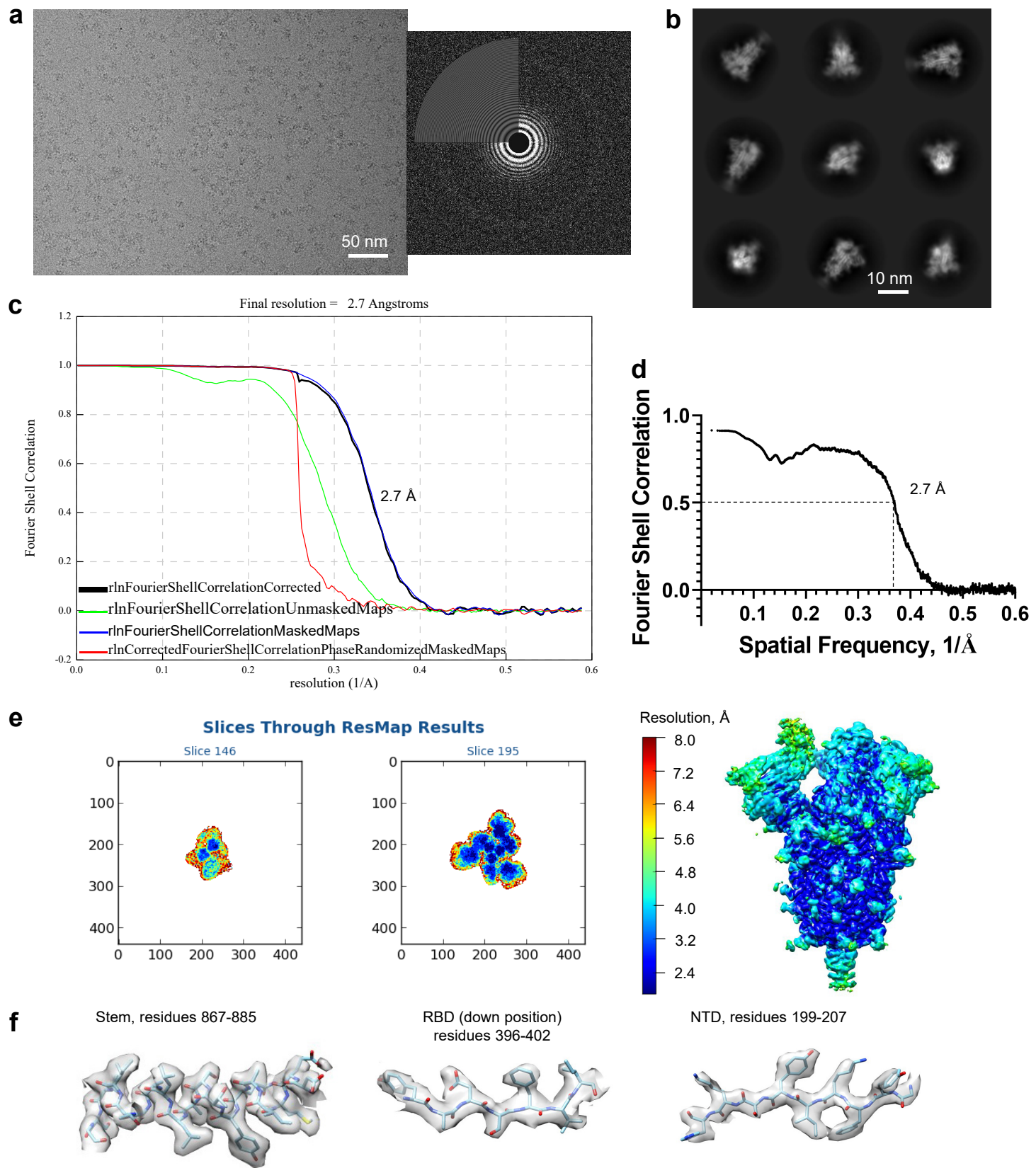
Extended Data Figure 4 | CryoEM with ACE2 at pH 7.4 and 5.5. e, The local resolution of each complex is represented. f, Cryo-EM data collection statistics for ACE2-bound structures are shown. (A single ACE2-bound structure of spike was recently described⁷⁵.)

Extended Data Figure 5



Extended Data Figure 5a | Cryo-EM data processing workflow leading to the consensus structure of SARS-CoV-2 spike at pH 5.5. Software packages are indicated in square brackets. (continued on next page)

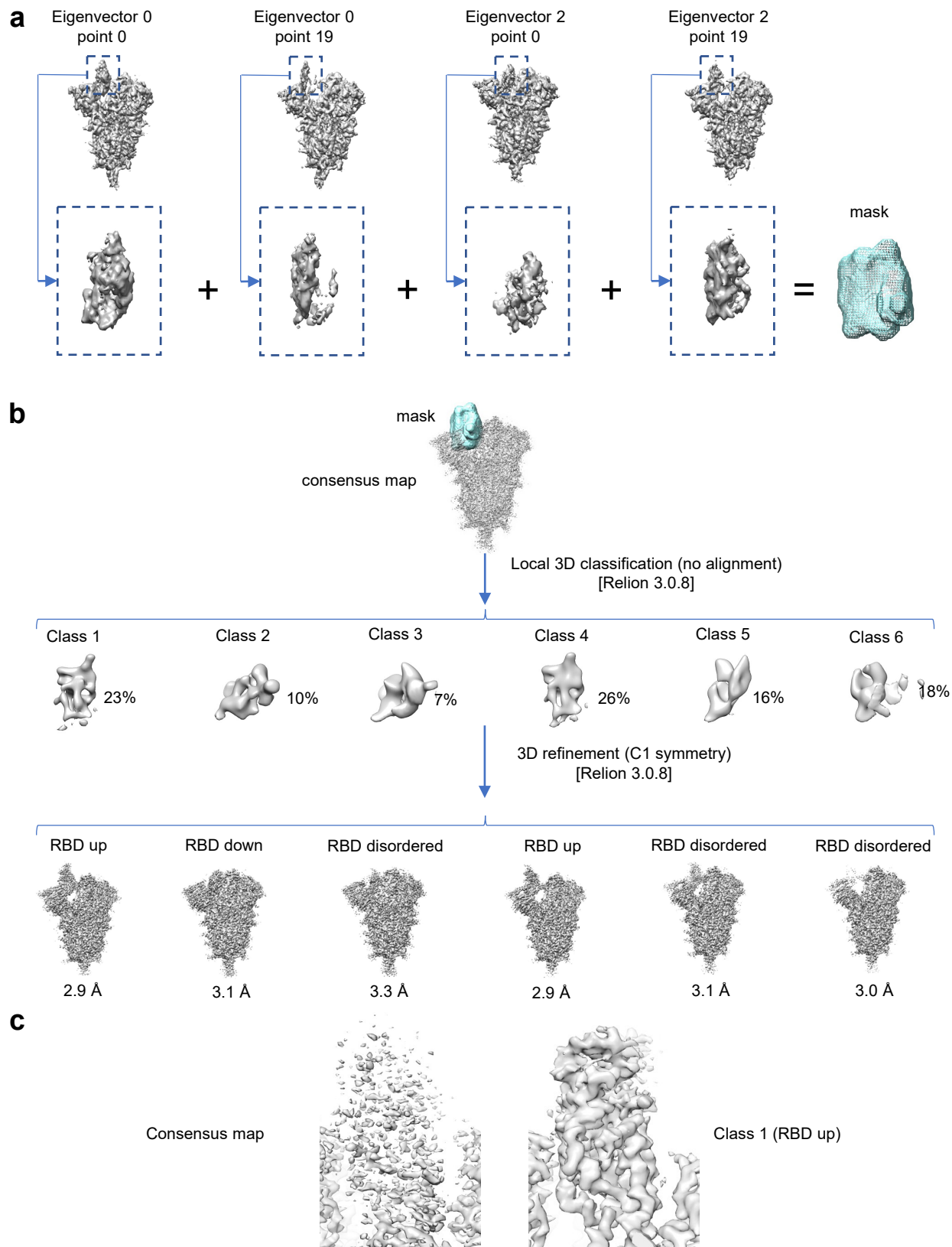
Extended Data Figure 5 (continued)



Extended Data Figure 5b | Validation of the consensus cryoEM map of SARS-CoV-2 spike at pH 5.5. a, Representative micrograph (left) and its power spectrum (right). **b,** Representative high-resolution 2D class averages. **c,** Gold-standard resolution data generated by Relion. At the 0.143 threshold, the resolution is 2.7 Å. **d,** Fourier shell correlation curve between the map and the atomic model. **e,** Results of local resolution analysis using ResMap. Left: Slices through the map at two different levels. Right: Map colored according to local resolution. **f,** Cryo-EM density in various regions.

(continued on next page)

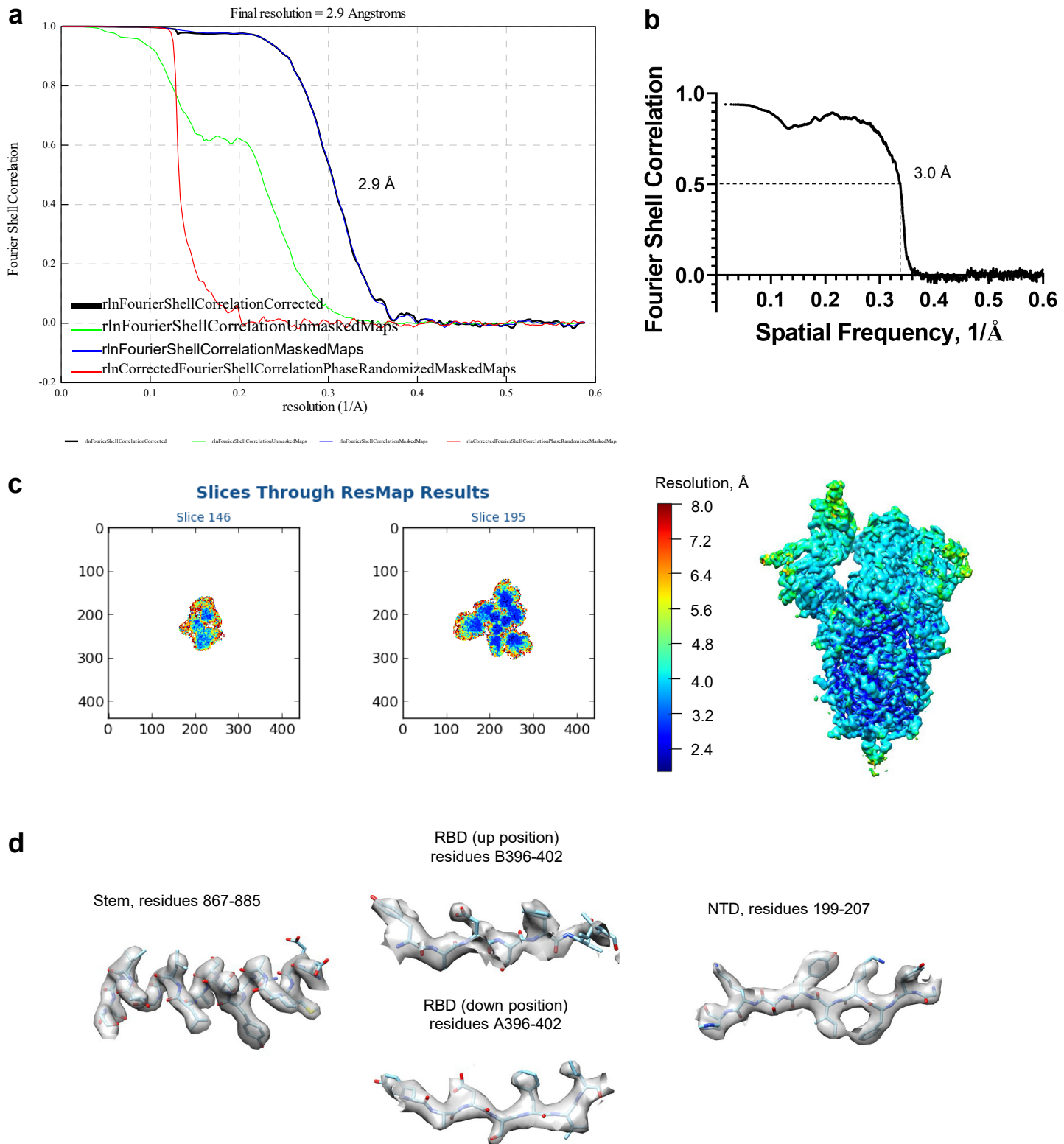
Extended Data Figure 5 (continued)



Extended Data Figure 5c | Analysis of heterogeneity in the RBD positions at pH 5.5. **a**, Extreme points (structures) along the trajectories defined by eigenvectors 0 and 2 in 3D variability analysis of the consensus structure were used to create a mask approximating the conformational space of the dynamic RBD domain. **b**, Local 3D classification of the consensus map within the mask defined in **a** produced six classes. Global 3D refinement of the corresponding subsets of particles resulted in two structures with the RBD in the up position, one with the RBD in the down position, and three with no defined position of the RBD. **c**, Comparison of the cryo-EM density corresponding to the RBD in the up position between the consensus map and the Class 1 map. The RBD is fully defined in the latter case.

(continued on next page)

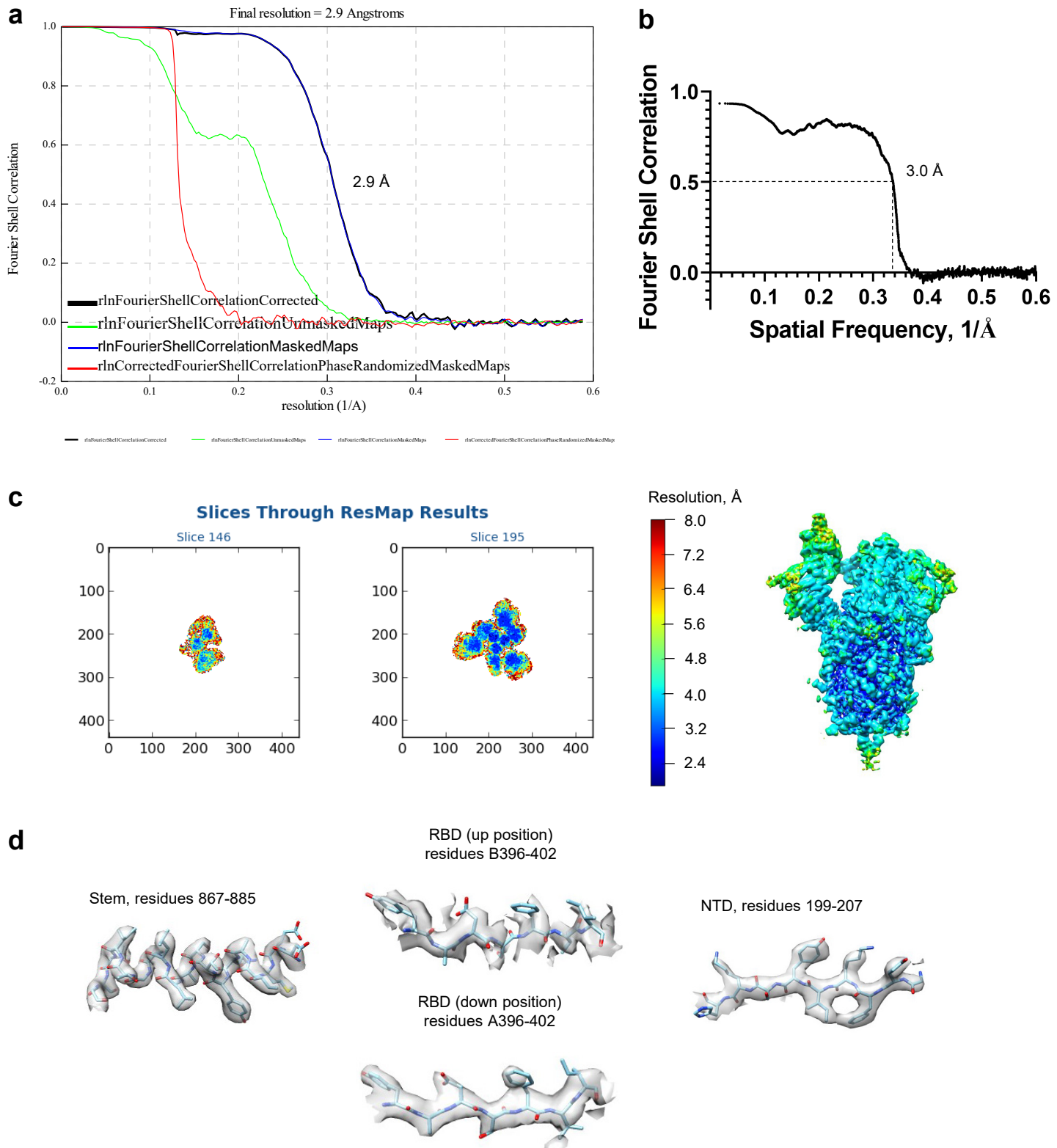
Extended Data Figure 5 (continued)



Extended Data Figure 5d | Validation of the cryo-EM map of SARS-CoV-2 spike at pH 5.5 with single RBD in the up position (conformation Up-1). **a**, Gold-standard resolution data generated by Relion. At the 0.143 threshold, the resolution is 2.9 Å. **b**, Fourier shell correlation curve between the map and the atomic model. **c**, Results of local resolution analysis using ResMap. Left: Slices through the map at two different levels. Right: Map colored according to local resolution. The RBD in the up position is fully resolved. **d**, Examples of cryo-EM density in various regions. The quality of the density for the RBD in the up position allowed building an atomic model for this domain.

(continued on next page)

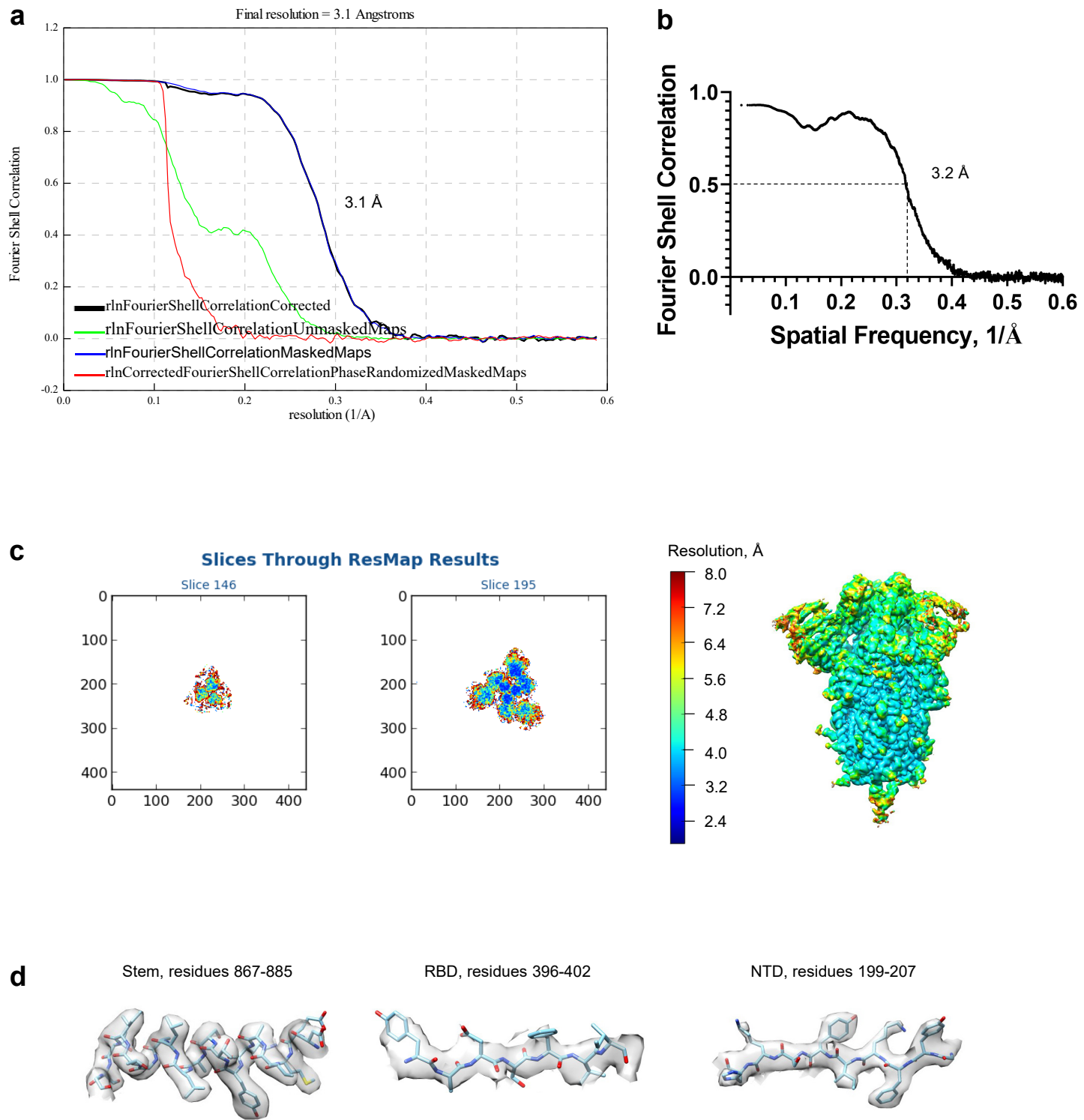
Extended Data Figure 5 (continued)



Extended Data Figure 5e | Validation of the cryo-EM map of SARS-CoV-2 spike at pH 5.5 with single RBD in the up position (conformation Up-2). **a**, Gold-standard resolution data generated by Relion. At the 0.143 threshold, the resolution is 2.9 Å. **b**, Fourier shell correlation curve between the map and the atomic model. **c**, Results of local resolution analysis using ResMap. Left: Slices through the map at two different levels. Right: Map colored according to local resolution. The RBD in the up position is fully resolved. **d**, Examples of cryo-EM density in various regions. The quality of the density for the RBD in the up position allowed building an atomic model for this domain.

(continued on next page)

Extended Data Figure 5 (continued)



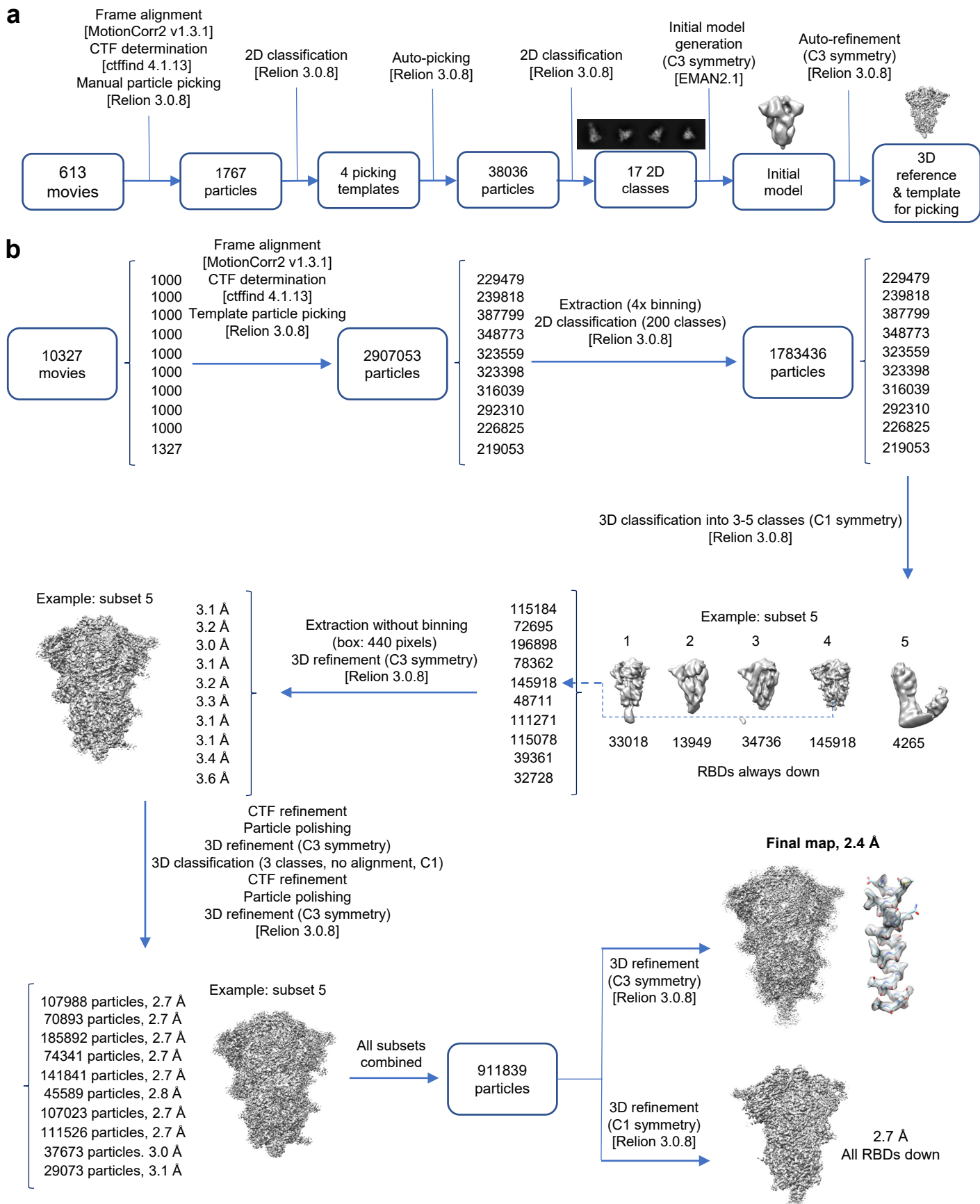
Extended Data Figure 5f | Validation of the cryo-EM map of SARS-CoV-2 spike at pH 5.5 with all RBDs in the down position. **a**, Gold-standard resolution data generated by Relion. At the 0.143 threshold, the resolution is 3.1 Å. **b**, Fourier shell correlation curve between the map and the atomic model. **c**, Results of local resolution analysis using ResMap. Left: Slices through the map at two different levels. Right: Map colored according to local resolution. **d**, Examples of cryo-EM density in various regions.

Extended Data Figure 5 (continued)

Extended Data Figure 5g | Cryo-EM data collection, refinement and validation statistics for structures determined at pH 5.5.

Structures	SARS-CoV-2 S pH 5.5 consensus map (EMD-xxxxx) (PDB xxxx)	SARS-CoV-2 S pH 5.5 RBD up-1 (EMD-xxxxx) (PDB xxxx)	SARS-CoV-2 S pH 5.5 RBD up-2 (EMD-xxxxx) (PDB xxxx)	SARS-CoV-2 S pH 5.5 RBD all-down (EMD-xxxxx) (PDB xxxx)
Data collection and processing				
Magnification				
105,000				
Voltage (kV)				
300				
Electron exposure (e-/Å ²)				
40				
Defocus range (μm)				
-1.25 to -2.5				
Pixel size (Å)				
0.85				
Symmetry imposed				
C1				
Initial particle images (no.)				
2,113,090				
Final particle images (no.)				
1,083,554				
Map resolution (Å)				
2.7				
FSC threshold				
0.143				
Map resolution range (Å)				
1.9-8.4				
Refinement				
Initial model used (PDB code)				
6VYB				
Model resolution (Å)				
2.7				
FSC threshold				
0.5				
Map sharpening <i>B</i> factor (Å ²)				
-72.3				
Model composition				
Non-hydrogen atoms				
25172				
Protein residues				
3120				
Ligands				
57				
Water				
-				
Model composition				
Non-hydrogen atoms				
25172				
Protein residues				
3120				
Ligands				
57				
Water				
-				
<i>B</i> factors (Å ²)(mean)				
Protein				
27.2				
Ligand				
45.3				
Water				
R.m.s. deviations				
Bond lengths (Å)				
0.009				
Bond angles (°)				
1.110				
Validation				
MolProbity score				
1.48				
Clash score				
2.22				
Poor rotamers (%)				
0.40				
Ramachandran plot				
Favored (%)				
92.0				
Allowed (%)				
7.9				
Disallowed (%)				
0.1				

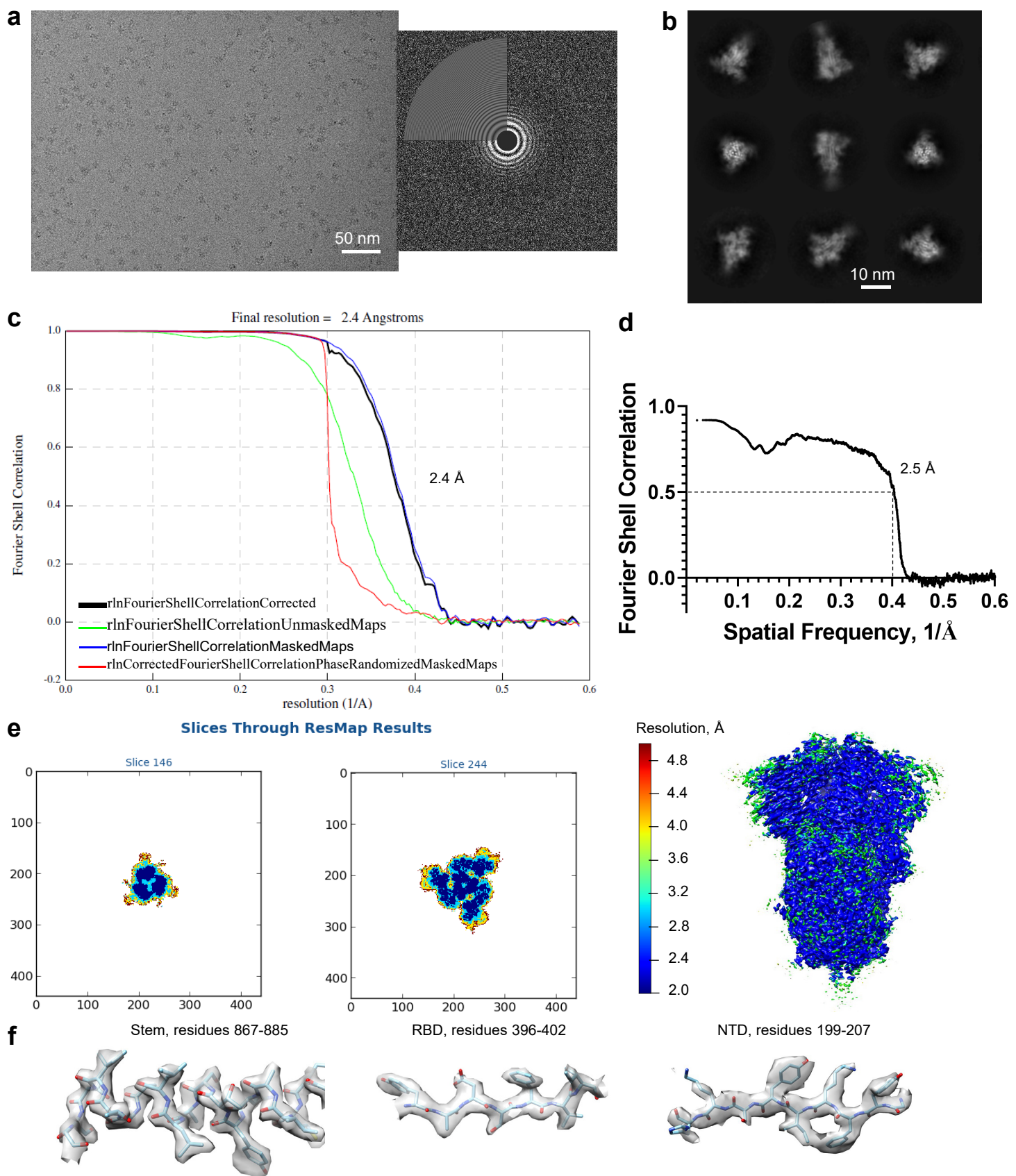
Extended Data Figure 6



Extended Data Figure 6a | Cryo-EM data processing workflow for SARS-CoV-2 spike at pH 4.0. **a**, generation of the initial 3D reference (also used as the 3D particle picking template). **b**, Steps of single particle analysis. Software packages are indicated in square brackets. RBD: receptor binding domain.

(continued on next page)

Extended Data Figure 6 (continued)



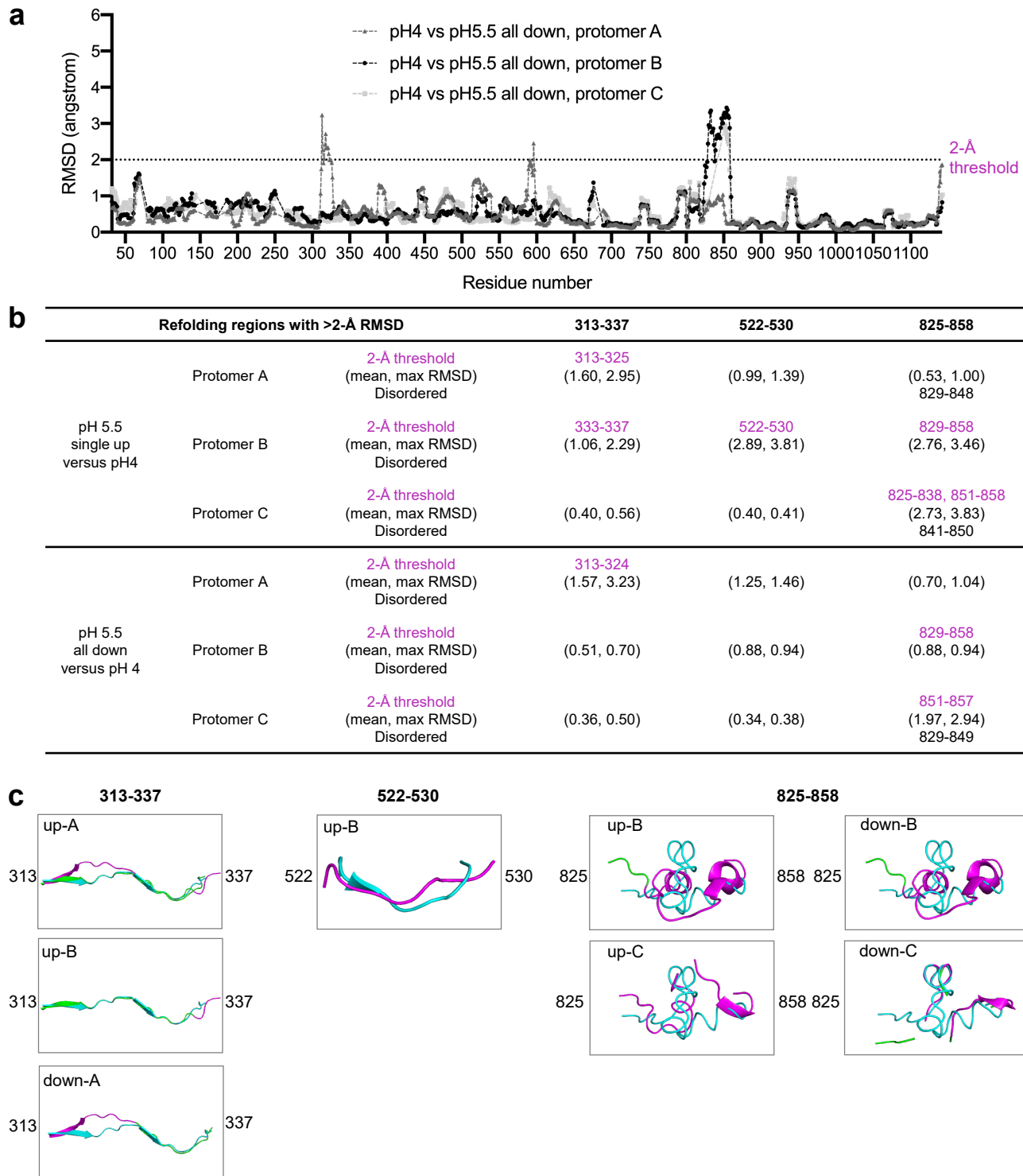
Extended Data Figure 6b | Validation of the cryoEM map of SARS-CoV-2 spike at pH 4.0 refined with C3 symmetry imposed. **a**, Representative micrograph (left) and its power spectrum (right). **b**, Representative high-resolution 2D class averages. **c**, Gold-standard resolution data generated by Relion. At the 0.143 threshold, the resolution is 2.4 Å. **d**, Fourier shell correlation curve between the map and the atomic model. **e**, Results of local resolution analysis using ResMap. Left: Slices through the map at two different levels. Right: Map colored according to local resolution. **f**, Examples of cryo-EM density in various regions.

Extended Data Figure 6 (continued)

Extended Data Figure 6c | Cryo-EM data collection, refinement and validation statistics for structure determined at pH 4.0.

Structure	SARS-CoV-2 Spike at pH 4.0 (EMD-xxxxx) (PDB xxxx)
Data collection and processing	
<hr/>	
Magnification	105,000
Voltage (kV)	300
Electron exposure (e-/Å ²)	40
Defocus range (μm)	-1.25 to -2.5
Pixel size (Å)	0.85
Symmetry imposed	C3
Initial particle images (no.)	2,907,053
Final particle images (no.)	911,839
Map resolution (Å)	2.4
FSC threshold	0.143
Map resolution range (Å)	1.8-4.8
<hr/>	
Refinement	
<hr/>	
Initial model used (PDB code)	6VXX
Model resolution (Å)	2.5
FSC threshold	0.5
Map sharpening <i>B</i> factor (Å ²)	-61.0
Model composition	
Non-hydrogen atoms	
Protein residues	
Ligands	
Water	
Model composition	25827
Non-hydrogen atoms	3163
Protein residues	NAG: 62
Ligands	252
Water	
<i>B</i> factors (Å ²)(mean)	44.7
Protein	67.2
Ligand	20.2
Water	
R.m.s. deviations	
Bond lengths (Å)	0.007
Bond angles (°)	1.033
Validation	
MolProbity score	1.32
Clash score	1.18
Poor rotamers (%)	0.14
Ramachandran plot	
Favored (%)	94.4
Allowed (%)	5.4
Disallowed (%)	0.1

Extended Data Figure 7



Extended Data Figure 7 | Details of refolding region analysis. **a**, Identification of refolding regions through rmsd analysis with a 11-residue sliding window comparing pH 5.5 all-down and 4.0 structures, with rmsds calculated for backbone atoms. **b**, Statistics on refolding analysis comparing pH 4.0 structure to pH 5.5 single-up and pH 5.5 all-down structures respectively, including regions with greater than 2-Å rmsd, mean and maximum rmsd, and disordered residues in pH 5.5 structures, for three refolding regions. **c**, Alignment of refolding regions between comparing pH 4.0 structure and pH 5.5 structures. pH 4 structures are colored in cyan. pH 5.5 structures are colored in green, with the residue regions with >2-Å rmsd colored in magenta.

Extended Data Figure 8

		pH5.5		pH 5.5 single-up conformation 1		pH 5.5 single-up conformation 2		6vxx		6vyb		
		All-down		B-up		B-up		All-down		B-up		
		Angle (°)	Displacement (Å)	Angle (°)	Displacement (Å)	Angle (°)	Displacement (Å)	Angle (°)	Displacement (Å)	Angle (°)	Displacement (Å)	
pH4	A	NTD	0.8	0.4	0.3	0.6	1.1	0.5	6.2	6.2	6.5	6.2
		RBD	1.2	0.6	2.4	1.3	2.7	1.4	4.6	5.6	6.4	5.3
		SD1	16.4	2.8	16.7	2.8	16.7	2.8	3.5	3.1	4.2	2.8
		SD2	1.3	0.2	1.2	0.2	1.2	0.3	4.3	4.7	3.2	4.7
		S2	0.2	2.9	0.3	1.3	0.3	1.3	0.1	1.8	0.2	1.9
	B	NTD	11.9	8.2	11.9	8.8	11.7	8.6	7.2	6.3	8.0	7.8
		RBD	3.2	1.0	64.9	22.8	67.0	25.5	4.7	4.6	66.9	22.3
		SD1	7.9	2.8	12.5	4.4	14.3	4.9	3.4	3.0	12.1	5.9
		SD2	8.3	2.1	9.1	2.8	9.9	2.7	4.3	4.7	5.7	4.8
		S2	0.4	2.7	0.3	0.2	0.2	0.2	0.1	2.1	0.1	2.0
	C	NTD	7.9	5.1	10.7	5.1	11.5	6.4	7.3	6.3	1.2	8.1
		RBD	0.6	0.4	1.2	0.2	1.7	0.6	4.5	5.7	3.4	6.8
		SD1	0.4	0.5	1.1	0.9	1.0	1.1	3.5	3.0	2.6	3.1
		SD2	4.7	0.9	7.0	0.8	8.5	1.0	4.3	4.8	7.6	4.6
		S2	0.1	1.7	0.2	1.8	0.2	0.8	0.1	2.1	0.1	2.5
pH5.5-1	A	NTD	0.6	0.1			0.5	0.3			5.7	6.0
		RBD	1.5	0.8			0.9	0.2			5.7	4.8
		SD1	1.7	0.0			0.8	0.1			11.2	3.5
		SD2	0.1	0.1			0.4	0.1			3.1	4.6
		S2	0.1	4.0			0.0	0.0			0.1	0.8
	B-up	NTD	1.3	0.6			0.6	0.1			6.2	4.6
		RBD	62.4	22.4			8.0	5.0			5.7	7.9
		SD1	4.8	1.7			2.5	0.6			1.1	1.7
		SD2	0.7	0.8			0.5	0.1			4.0	4.1
		S2	0.0	2.7			0.1	0.1			0.1	2.0
	C	NTD	4.3	0.9			2.2	1.4			2.5	4.3
		RBD	0.7	0.3			0.5	0.4			2.4	6.7
		SD1	0.9	0.4			0.9	0.3			3.4	2.5
		SD2	2.9	0.3			1.3	0.4			1.5	4.4
		S2	0.3	2.8			0.1	1.0			0.2	0.8
pH5.5-2	A	NTD	0.7	0.3							5.5	5.8
		RBD	1.8	1.0							4.9	4.8
		SD1	1.8	0.1							12.0	3.4
		SD2	0.4	0.1							2.8	4.5
		S2	0.1	4.0							0.1	0.8
	B-up	NTD	1.5	0.5							6.3	4.6
		RBD	64.6	25.0							2.9	7.1
		SD1	6.1	2.2							2.7	1.5
		SD2	0.8	0.7							3.6	4.0
		S2	0.2	2.8							0.2	2.0
	C	NTD	4.1	1.3							0.6	4.2
		RBD	1.3	0.6							1.9	6.4
		SD1	0.9	0.7							2.6	2.2
		SD2	3.2	0.2							0.4	4.4
		S2	0.2	2.1							0.2	1.7



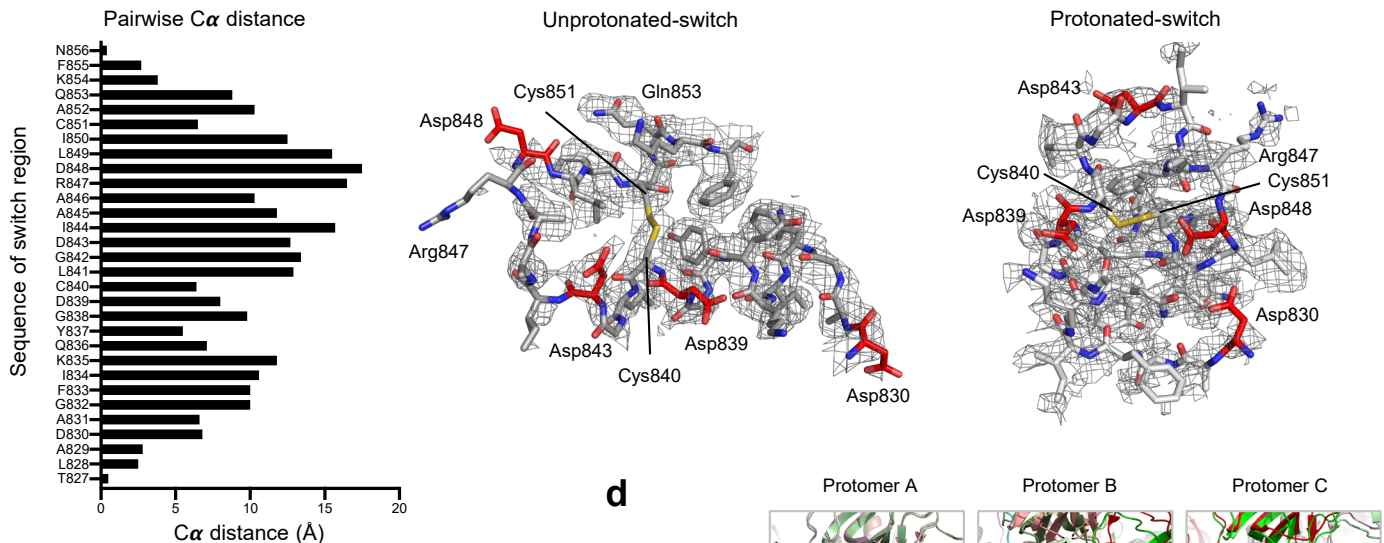
Extended Data Figure 8 | Domain movements between single-RBD up (pH 5.5) and all-RBD down (pH 4.0) structures.
 Movements are expressed as rotation angles and displacements between corresponding domains in the pH 5.5 and pH 4.0 structures. Structures were first superimposed in the S2 domain with residues 728 to 1140, domains within the same superimposed protomer were compared.

Extended Data Figure 9

a

		Pairwise RMSD (Å) of residue 825-858									
		Unprotonated-switch			Protonated-switch						
		pH5.5 up1, B	pH5.5 up1, C	pH5.5 up2, B	pH5.5 up2, C	pH5.5 down, B	pH4, A	pH4, B	pH4, C	pH5.5 down, A	
Unprotonated-switch	pH5.5 up1, B (shown below)	0	2.349	0.599	2.372	0.382	6.903	6.836	7.182	7.214	
	pH5.5 up1, C	2.349	0	2.376	1.56	2.398	5.66	5.782	6.405	6.278	
	pH5.5 up2, B	0.599	2.376	0	2.41	0.622	6.805	6.75	7.081	7.114	
	pH5.5 up2, C	2.372	1.56	2.41	0	2.4	5.91	6.007	6.588	6.459	
	pH5.5 down, B	0.382	2.398	0.622	2.4	0	6.866	6.824	7.167	7.21	
Protonated-switch	pH4, A	6.903	5.66	6.805	5.91	6.866	0	1.067	1.223	1.462	
	pH4, B (shown below)	6.836	5.782	6.75	6.007	6.824	1.067	0	0.98	1.003	
	pH4, C	7.182	6.405	7.081	6.588	7.167	1.223	0.98	0	1.087	
	pH5.5 down, A	7.214	6.278	7.114	6.459	7.21	1.462	1.003	1.087	0	

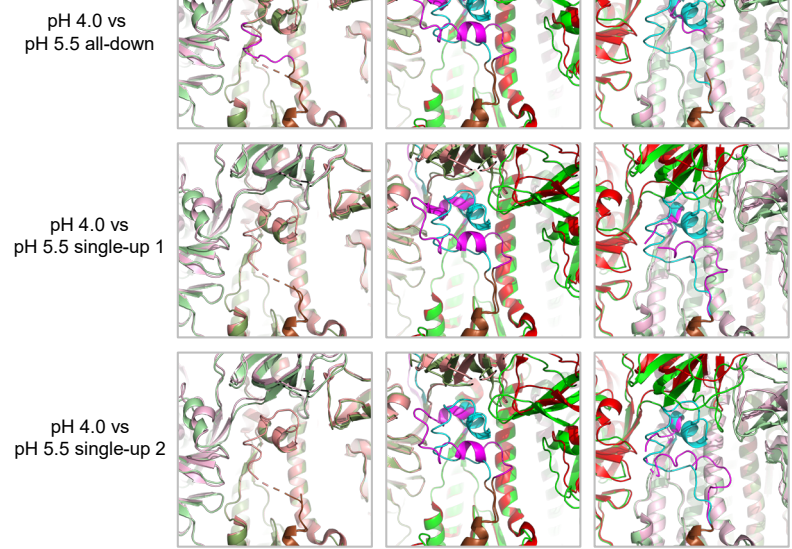
b Cryo-EM densities and conformation of the switches in protomer B of the pH 5.5 and pH 4.0 structures



c Inter- and intra-protomer interface areas for switches

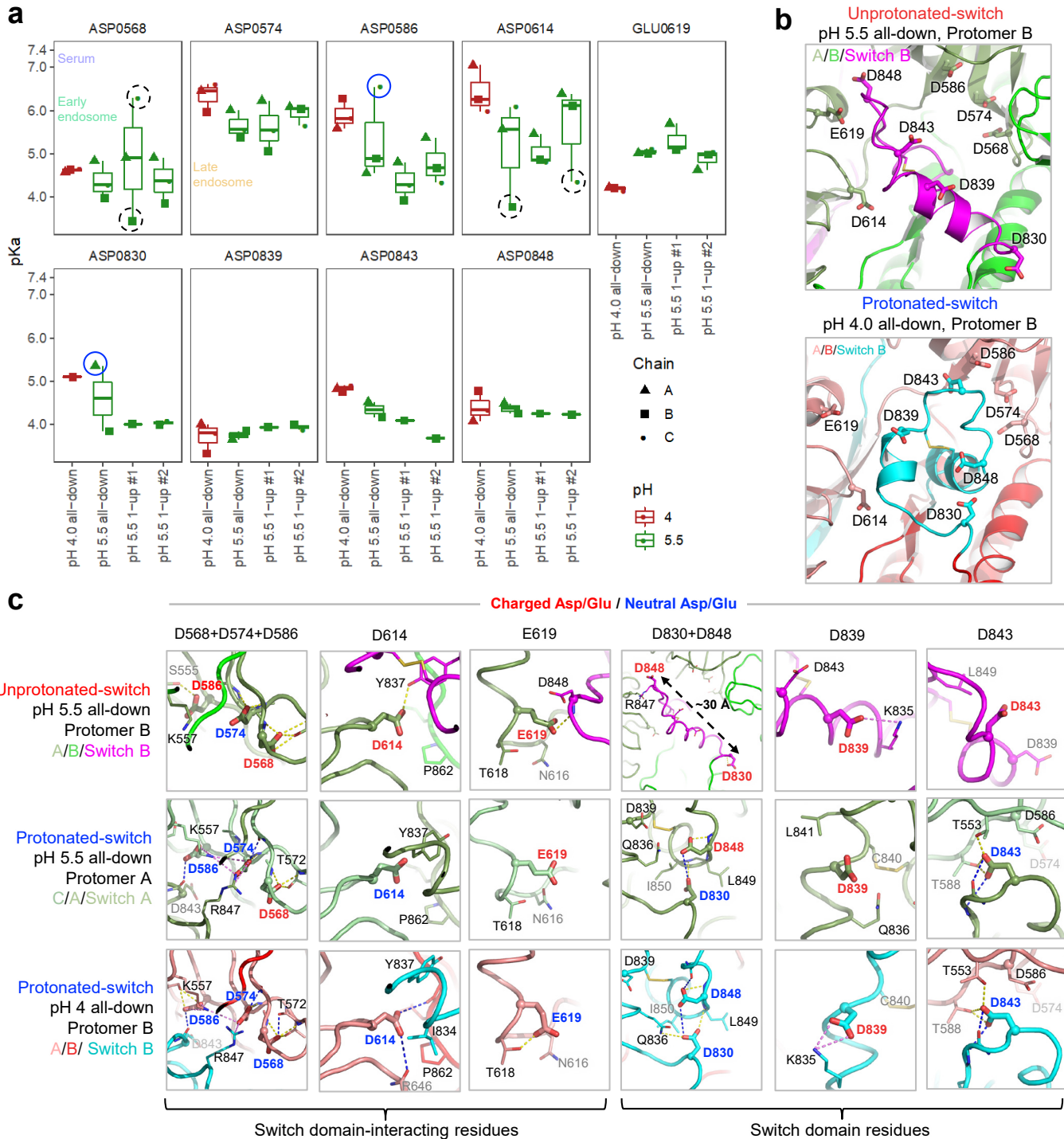
Buried surface area (Å ²)	Switch A			Switch B			Switch C					
	Inter-protomer on C	Intra-protomer on A	Inter-protomer on A	Intra-protomer on B	Inter-protomer on B	Intra-protomer on C	Inter-protomer on C	Intra-protomer on A	Intra-protomer on B	Intra-protomer on C		
pH 4.0	SD1	368.67	NTD	75.67	SD1	350.92	NTD	80.77	SD1	364.03	NTD	79.69
	SD2	201.77	S2	458.35	SD2	165.08	S2	465.75	SD2	209.17	S2	459.62
	Asp614	90			Asp614	71.6			Asp614	84.9		
	Total	568.5		534		515.6		547		573.2		539.3
pH 5.5-1	SD1	116.94	NTD	0	SD1	151.96	NTD	2.5	SD1	227.06	NTD	0
	SD2	82.16	S2	349.5	SD2	296.81	S2	534.17	SD2	95.06	S2	537.5
	Asp614	18.9			Asp614	73.8			Asp614	44.6		
	NAG1309				NAG1309	53.1			NAG1309	10		
pH 5.5-2	Total	199.1		349.5		501.87		536.6		332.12		537.5
	SD1	139	NTD	0	SD1	145.58	NTD	9.5	SD1	239.47	NTD	0
	SD2	81.38	S2	367.3	SD2	222.8	S2	547.4	SD2	130	S2	524.3
	Asp614	22.7			Asp614	70.4			Asp614	56.4		
NAG1309					NAG1309	36			NAG1309			
	Total	220.4		367.3		404.38		556.9		360.47		524.3

d



Extended Data Figure 9 | The pH-switch domain. a, Pairwise rmsd between switch regions (residues 825-858) from different protomers. Of the 12 protomers determined in this study, only 9 had at least 17-ordered residues and were included in this pairwise-rmsd analysis, with rmsds of less than 2.5 Å shaded grey. A switch region structure resembling the protonated-switches has been described for a murine coronavirus, PDB: 6VSJ³⁶, with structurally similar switches also recently described for SARS-CoV-2 structures^{24,50,75,76}). b, Pairwise C α distance of the refolding region in pH 5.5 and pH 4.0, and EM density map of the refolding 830-855 region in protomer B of the pH 5.5 and pH 4.0 structures. Asp residues are colored red, and Cys residues are colored yellow. c, Inter- and intra-protomer interaction surface areas by the pH-switches in the pH 5.5 and pH 4.0 structures. d, Comparison of the refolding region in pH 5.5 and pH 4.0 structures. The structures were superposed on S2 region and conformation of the switch in each protomer of the three pH 5.5 structures were compared with corresponding ones in pH 4.0. Refolding regions are colored magenta and cyan for pH 5.5 and pH 4.0 structures, respectively, and as defined in Extended Data Figure 7.

Extended Data Figure 10



Extended Data Figure 10 | pKa calculations for the pH-switch domain. **a**, PROPKA-calculated pKas for titratable residues in and near the 825–858 pH-dependent switch domain region are plotted for all modeled conformations in each structure, disordered regions excluded. Reference lines are shown for the structure pHs (5.5 and 4.0) as well as typical pH values for serum (7.4), early endosome (6.0) and late endosome (4.5), colored as in Figure 1a. Residues with noticeably higher or lower calculated pKas compared to other conformations at the same pH are circled, and can be attributed to either adoption of the protonated-switch conformation by Protomer A in the pH 5.5 all-down structure (blue circles, see panel c, middle row); or proximity to disordered regions in the structures (black dashed circles). **b**, Individual pH switch domain conformations from the indicated pH 4.0 and pH 5.5 structures, with the switch domain and surrounding protomers colored as indicated. Residues from **a** are shown as sticks with Ca as spheres. **c**, Close-up views of Asp residues from **(a-b)**, indicating changes in chemical environment for each residue. Highlighted residue labels are colored based on pKa-based dominant protonation state, with charged Asp/Glu in red and neutral (protonated) Asp/Glu in blue, and are shown as thick sticks, with residues within 4 Å shown as thin sticks. Dashed lines indicate hydrogen bonds (yellow) and salt bridge interactions (violet), with hydrogen bonds that require Asp protonation indicated in blue. The pKa shifts between unprotonated- and protonated-switch conformations define a pH-dependent stability gradient that favors the protonated-switch form at lower pHs⁷⁷. However, other factors such as global conformational constraints may also play a role in favoring one conformation over another. Indeed, a number of SARS-CoV-2 spike structures^{24,50,75,76} have recently been reported which contain switch domain conformations at physiological pH that are similar yet clearly distinct from the low-pH protonated-switch conformation we report.